

Article

Determination of Plant Nitrogen Content in Wheat Plants via Spectral Reflectance Measurements: Impact of Leaf Number and Leaf Position

Georg Röhl ^{1,*} , Jens Hartung ² and Simone Graeff-Hönninger ¹ 

¹ Department of Agronomy, Institute of Crop Science, University of Hohenheim, 70599 Stuttgart, Germany; Simone.graeff@uni-hohenheim.de

² Department of Biostatistics, Institute of Crop Science, University of Hohenheim, 70599 Stuttgart, Germany; jens.hartung@uni-hohenheim.de

* Correspondence: georg.roell@uni-hohenheim.de; Tel.: +49-711 459-22380

Received: 9 September 2019; Accepted: 22 November 2019; Published: 26 November 2019



Abstract: The determination of plant nitrogen (N) content (%) in wheat via destructive lab analysis is expensive and inadequate for precision farming applications. Vegetation indices (VI) based on spectral reflectance can be used to predict plant N content indirectly. For these VI, reflectance from space-borne, airborne, or ground-borne sensors is captured. Measurements are often taken at the canopy level for practical reasons. Hence, translocation processes of nutrients that take place within the plant might be ignored or measurements might be less accurate if nutrient deficiency symptoms occur on the older leaves. This study investigated the impact of leaf number and measurement position on the leaf itself on the determination of plant N content (%) via reflectance measurements. Two hydroponic experiments were carried out. In the first experiment, the N fertilizer amount and growth stage for the determination of N content was varied, while the second experiment focused on a secondary induction of N deficiency due to drought stress. For each plant, reflectance measurements were taken from three leaves (L1, L2, L3) and at three positions on the leaf (P1, P2, P3). In addition, the N content (%) of the whole plant was determined by chemical lab analysis. Reflectance spectrometer measurements (400–1650 nm) were used to calculate 16 VI for each combination of leaf and position. N content (%) was predicted using each VI for each leaf and each position. Significant lower mean residual error variance (MREV) was found for leaves L1 and L3 and for measurement position on P3 in the N trial, but the difference of MREV between the leaves was very low and therefore considered as not relevant. The drought stress trial also led to no significant differences in MREV between leaves and positions. Neither the position on the leaf nor the leaf number had an impact on the accuracy of plant nitrogen determination via spectral reflectance measurements, wherefore measurements taken at the canopy level seem to be a valid approach.

Keywords: wheat; spectrometer; nitrogen content; hydroponics; nitrogen treatments; growth stages; vegetation index

1. Introduction

Nitrogen (N) is a key plant nutrient commonly applied to increase yield and crop quality in agricultural systems [1]. However, the production of nitrogenous fertilizer creates large amounts of greenhouse gases [2]. Environmental pollution can also occur after excessive nitrogen application if the applied fertilizer amounts exceed plant demand [3]. Under unfavorable conditions, potential greenhouse gases can escape from soils or are transported to groundwater through leaching [4]. These side effects strongly depend on the amount of N fertilizer applied [5]. In Europe, the Water

Framework Directive [6] and Nitrates Directive [7] joined forces to lower the leaching potential. This is accomplished by reducing the N amount applied and by maintaining the right amount of N under different growing conditions (drought, or well-saturated soil, for example).

Over the last 30 years, concepts of precision farming (PF) [8] have been developed that help farmers to understand yield variability within their fields in order to adjust N application. Generally, PF uses different technologies like global positions systems, yield mapping, soil conductivity measurements [9] or non-contact spectral sensors for monitoring and determination of e.g., N status of different field crops [8]. These spectral sensors are based on the principle of reflectance and changes of electromagnetic radiation between 300 and 2500 nm [10] and can be ground-borne, airborne, or space-borne [11]. Space-borne sensors are widely available [12], but data collection is affected by clouds, poor atmospheric conditions, and has to cope with atmospheric perturbation [13]. In addition, they suffer from low spectral and spatial resolution (10–60 m) [14–16]. The closer the sensor to the target, the higher the spatial resolution [17]. This is one reason why an unmanned aerial vehicle (UAV)-based, or vehicle-mounted, sensors are mainly used in agriculture (resolution 0.01 m or less) [17,18]. However, these devices also still depend on environmental conditions like wind speed, rain, or changing cloud coverage [19]. Nevertheless, the advantage is an image acquisition where measurement date and resolution can be more influenced by the user compared to satellite images. The applications range from the detection of within-field variability for yield predictions to monitoring of water- or nitrogen stress [20–22]. Several commercialized products like the Yara N-Sensor, Fritzmeier Isaria, Greenseeker™ RT 200, or Crop Circle ACS-430 are available, which are measuring the reflectance at canopy level [23]. This leads to two challenges:

The first challenge is to distinguish between soil and plant reflectance signatures [24]. Soil reflectance is affected by soil moisture, organic matter, clay minerals, or iron oxides [25]. The differentiation between soil and plants is mainly realized by using indices that adjust for soil effects [26]. The difficulty of applying such indices is the compensation for different soil albedos, which change between soil types [27]. When using remote sensing instruments, leaf reflectance is always affected by the lower leaves and the soil background, which leads to interferences. Therefore, measured reflectance in an open field is always a mixture of different diffuse reflected light and never an isolated reflectance signal, which may lead to a reduction in overall accuracy.

However, the application of these spectral indices requires a certain ground coverage of the plant to overlay soil reflectance. Hence, the application of these indices is limited to certain growing periods [12,28]. In early growing stages, when the plant has low ground cover, no sensors can be used as the soil reflectance dominates the image [29]. Later in the growing season, a saturation of indices and reflectance values makes the prediction of N status difficult [30].

The second challenge is to distinguish between different parts of the plant. Most studies focused on chlorophyll and N content of the leaves or canopy [31] and therefore did not consider the actual crop's N content, which would be more desirable for decision support systems in PF [32]. The N content within a plant is assumed to be higher in younger leaves [23,24], while a higher sensitivity to N deficiency in older leaves was reported due to translocation processes [33,34]. Wang et al. [35] showed that ignoring vertical N distribution will lead to lower accuracy and limited practical value of crop N for remote sensing. To overcome the issue of vertical N distribution, remote sensing approaches have been adopted by several researchers [34–36]. Zhao et al. [36] generated spectral information with a spectroradiometer in winter wheat by changing view zenith angles from 0° to 60°. Angles of 20 to 30° gave information about the middle leaf layers, while angles of 0 to 20° and 30–60° measured mainly the upper leaves. However, a major drawback of this approach is that each measurement contains some mixed information of all the different layers [36].

This raised the question, on which leaf layer, and at which location on the leaf itself remote sensing measurements have to be carried out to determine the N content of a plant. Measurement at canopy level has to be considered as satisfying so far if different leaves, varying leaf ages, and stress levels lead to a similar reflectance. To the best of our knowledge, there is no publication investigating the influence of the leaf layer and position of the measurement on the leaf for cereal plants. Gara et al. [37] tested spectral reflectance on different short shrubs and showed the need to account for vertical heterogeneity.

Thus, the aim of this study was to investigate a) on which leaf layer and b) at what position on the leaf itself reflectance measurements should be taken from. These measurements were then used to determine the N content (%) of the wheat plant via a range of published VI while validating the data with chemically determined N content (%).

2. Materials and Methods

2.1. Plant Growth Conditions and Experimental Design

Two hydroponic greenhouse experiments were carried out to predict N content from wheat plants (*Triticum aestivum* L.) of the cultivar “Zenon” based on spectral measurements. To achieve this goal, direct destructive lab measurements of nitrogen content (%) of whole plants and indirect spectral reflectance measurements from three positions on three leaves of the same plant were taken. In both experiments, growing conditions in the greenhouse were set at 16/8 h day/night cycle with 400–500 $\mu\text{mol m}^{-2} \text{s}^{-1}$ and 20/18 °C day/night temperature. Plants were seeded in the sand and grown for two weeks. Afterward, plants were transferred to a modified Hoagland solution [38], which was continuously aerated and replaced twice a week and contained the following macro- and micronutrients in both trials: 10.0 mM CL, 7.5 mM Ca, 2.0 mM N, 1.2 mM K, 1.1 mM S, 0.6 mM Mg, 0.2 mM P, and 0.4 mM Fe (EDTA), 1.0 μM B, 0.5 μM Zn, 2.0 μM Mn, 0.3 μM Cu, 0.04 μM Mo. The concentration of the nutrient solution was gradually increased from 20% to 100% over seven days. The two experiments varied in the additional treatment factors added. In the nitrogen trial, different levels of nitrogen nutrition status were used. In the drought stress trial, different levels of water stress were induced.

2.1.1. Nitrogen Trial

In the nitrogen trial, the nitrogen fertilizer amount, and the growth stage in which the final spectral measurements took place were varied. For the former, seven different levels of N fertilizer amounts were used (with 0 mM, 0.25 mM N, 0.50 mM N, 0.75 mM N, 1 mM N, 1.5 mM N, 2.00 mM N) and applied in four replicates according to a randomized complete block design (Figure 1). This factor corresponded to the main plot factor. In total, 28 pots were used. Within each pot, five planting positions existed. At each position, a single plant was planted. A total of 140 plants were planted and harvested later (Figure 1). As plants were harvested at different growth stages, the growth stage factor corresponded to the sub-plot factor, as the randomization of the growth stage occurs within the pot. At harvest, the N content was measured by chemical lab analysis. Additionally, three spectrometer measurements from each of the last three fully developed leaves were taken directly before the harvest of each plant. This resulted in a total of 1260 reflectance measurements.

As in trials with different growth stages, the growth stage effect is confounded with either the planting date or the harvest date, a more complex design using planting dates and harvest dates as blocking factors were used. More details, a complete field plan, and a detailed description can be found in the Appendix A.

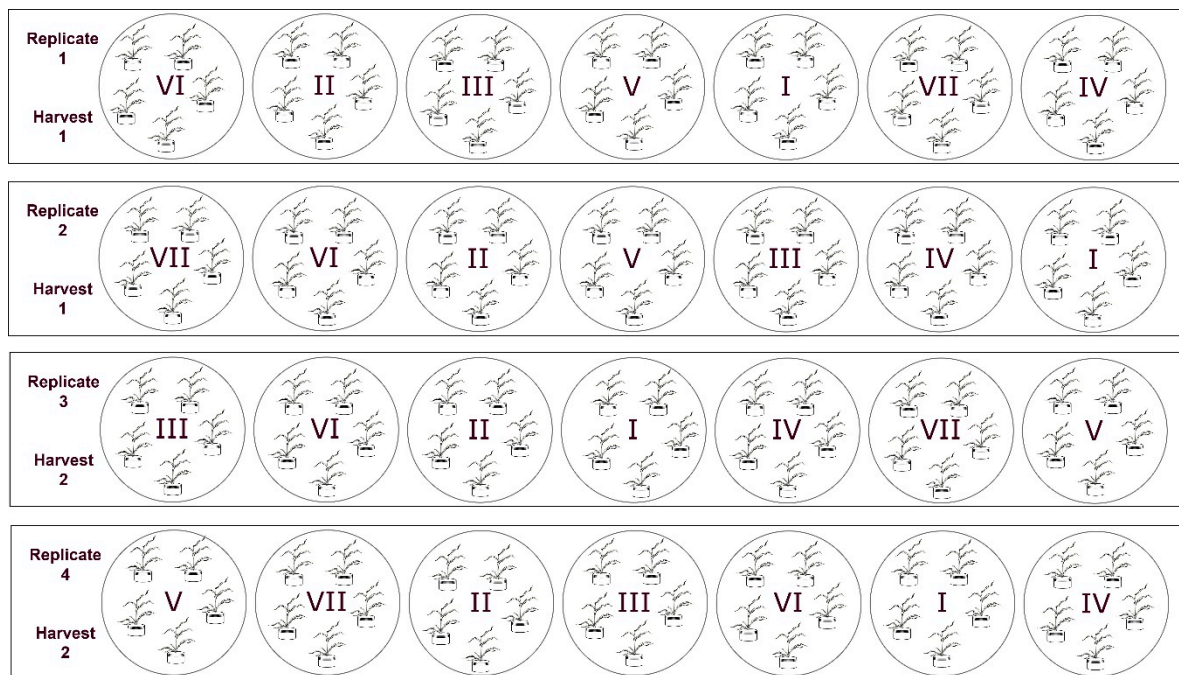


Figure 1. Experimental design of the nitrogen fertilizer trial. I–VII represents the pots of the corresponding nitrogen levels (0 mM N–2.0 mM N).

2.1.2. Drought Stress Trial

To apply drought stress to the hydroponic trials, four levels of polyethylene glycol (PEG 6000) were applied according to a randomized complete block design with three replicates. One replicate consisted of four pots with four plants per pot. Plants here correspond to repeated measures. All plants were transferred to the hydroponic solution at the same time. After one week of growing under the same conditions, the given polyethylene glycol levels (0 g l^{-1} ; 36 g l^{-1} ; 72 g l^{-1} ; 144 g l^{-1}) were applied. The N concentration was kept constant at 2.00 mM N in all pots. After 23 days, spectrometer reflectance measurements for each combination of plant, leaf, and position (resulting in 434 measurements) were taken and harvesting was performed. Plants were then bulked per pot, and N content was determined for each pot resulting in twelve N content values. This experiment was used to test the effect of drought stress on spectral reflectance combined with an assumed N deficit due to drought stress. At the highest drought level, it was not possible to measure the L3 of each plant due to strong leaf rolling. Therefore, L3 was excluded from the evaluation in this experiment.

2.2. Spectral Reflectance Measurements

Leaf reflectance measurements were conducted using a halogen light source (HL-2000-HP-FHSA, Ocean Optics, Germany) and connected to an integrating sphere (ISP-30-6-R, Ocean Optics, Germany) to keep the measurement conditions constant. The integrating sphere was connected via bifurcated fiber (QBIF400-MIXED, Ocean Optics, Germany) to allow simultaneous measurements of two spectrometers for the wavelength range 200–1025 nm (FLAME-S-XR1-ES, Ocean Optics, Germany) and for the wavelength range 900–1700 nm (NQ512-1.7, Ocean Optics, Germany) (Figure 2).

Due to a low signal to noise ratio at both ends of the spectrum, there was an effective range of 400–950 nm at a spectral resolution of 0.4 nm for the FLAME-spectrometer and an effective range of 950–1650 nm at a spectral resolution of 1.5 nm for the NQ512-1.7 spectrometer. The integration time was adjusted at the white standard (Spectralon WS-1-SL, Ocean Optics, Germany) to ensure that enough light reached the sensor. It was set to 80%–95% of light saturation and adjusted for both spectrometers separately and gave the highest signal to noise ratio.

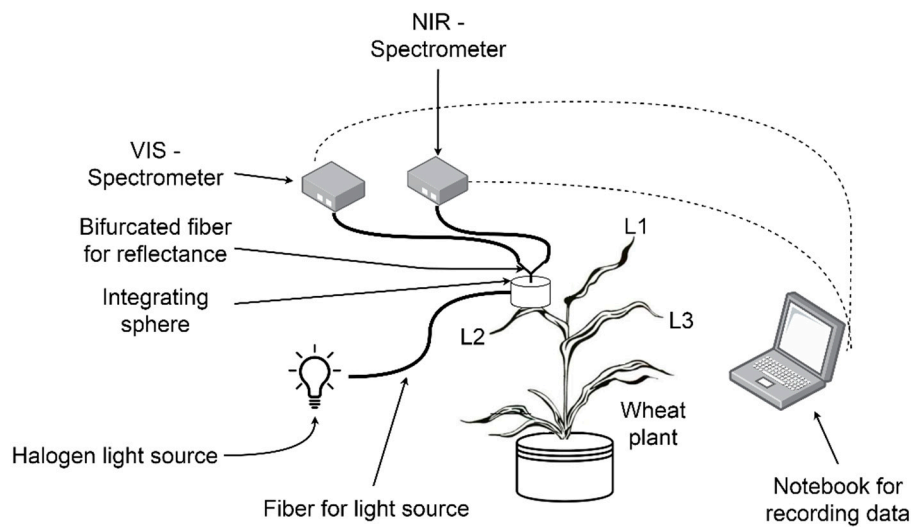


Figure 2. Setup scheme for leaf reflectance measurements under controlled conditions. The numbers indicate the order of leaves 1–3.

Leaf reflectance was calculated as a ratio between the reflected energy of the leaf and the incident energy of the light source. This incident energy was determined by using the reference measurement of the white standard.

The measurement was performed by placing the opening of the integrating sphere on the different leaves and leaf positions (Figure 2). The last fully developed leaf of the main stem was considered as the youngest leaf (L1) and was measured at three positions: leaf tip (P1), leaf center (P2), leaf base (P3) (Figure 3). The same procedure was performed for leaf two (L2) and three (L3). Note, the counting of the leaves always started at the youngest fully developed leaf downwards (Figure 3).

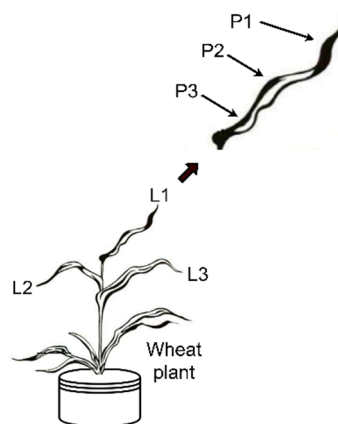


Figure 3. Scheme of the spectral measurements on the plant. P1–P3 indicates the measurement on the leaf and L1–L3 indicates the leaf number. Measurements on L2 and L3 were performed in the same way as indicated for L1.

2.3. Crop Measurements and Harvesting

After the reflectance measurements, the growth stage rating was performed based on the Zadocks scale [39] for each plant separately. Finally, plants were harvested by cutting off the stem from the roots. The stem was weighed (3100 S-G, Sartorius AG, Göttingen, Germany ± 0.01 g) and immediately dried for two days at 60 °C in a forced-air drier. After drying, the dry weight of the samples was determined; samples were ground using a hammer mill (0.5 mm, MM200, Retsch GmbH, Haan,

Germany). The chemical elementary analysis was performed, using a Vario Macro cube (Elementar Analysensysteme GmbH, Hanau, Germany) based on the method of Dumas [40].

2.4. Vegetation Indices (VI)

Information on spectral reflection measurements was explored using different VI. From a literature review, 16 VI (Table 1) with a significant correlation with plant N content or plant water content were selected and calculated for each leaf and position on each leaf [12,41,42].

Table 1. Common vegetation indices used in this study.

Index	Name	Formula	Reference
BNI	Blue nitrogen index	$\frac{R434}{(R496+R401)}$	[43]
CropSpec		$\left(\frac{R808}{R735} - 1\right) \cdot 100$	[44]
GNDVI	Green normalized difference vegetation index	$\frac{(R750-R550)}{(R750+R550)}$	[45]
HVI	Hyperspectral vegetation index	$\frac{R750}{R700}$	[29]
NDVI	Normalized difference vegetation index	$\frac{(R900-R680)}{(R900+R680)}$	[46]
NDWI	Normalized difference water index	$\frac{(R860-R1240)}{(R860+R1240)}$	[47]
NIRG	Near-infrared green ratio	$\frac{R780}{R550}$	[48]
NIRR	Near-infrared red ratio	$\frac{R780}{R700}$	[48]
NWI	Normalized water index	$\frac{(R970-R900)}{(R970+R900)}$	[49]
PRI	Photochemical reflectance index	$\frac{(R531-R570)}{(R531+R570)}$	[50]
PSRI	Plant senescence reflectance index	$\frac{(R680-R500)}{(R750)}$	[51]
REIP	Red-edge inflection point	$700 + 40 \cdot \frac{(R670+R780) / 2 - R700}{R740-R700}$	[52]
SIPI	Structure insensitive pigment index	$\frac{(R800-R445)}{(R800+R680)}$	[50]
SR 680	Simple ratio 680	$\frac{R800}{R680}$	[50]
SR 705	Simple ratio 705	$\frac{R680}{R705}$	[41]
VARI	Visible atmospherically resistant index	$\frac{(R550-R650)}{(R550+R650-R470)}$	[53]

2.5. Statistical Analysis (Mixed Model)

Data of the N trial were analyzed by a mixed model approach accounting for the two factors, nitrogen fertilizer treatment and growth stage, as well as the two blocking factors, the sowing date and harvest date (for more details of the experimental design see appendix).

The model can be described by:

$$y_{ijklmn} = \mu + \tau_m + \varphi_n + (\tau\varphi)_{mn} + h_i + s_j + r_k + t_{kl} + e_{ijklmn} \quad (1)$$

where y_{ijklmn} is the measured plant N content, μ is the intercept, τ_m is the fixed effect of the m th N treatment, φ_n is the fixed effect of the n th growth stage, and $(\tau\varphi)_{mn}$ the corresponding fixed interaction effect. h_i is the random block effect of the i th harvesting date, s_j is the random block effect of the j th sowing date, r_k is the fixed effect of the k th replicate, and t_{kl} is the random effect of the l th pot or main plot within the k th replicate. e_{ijklmn} is the error of observation y_{ijklmn} .

The model for the drought trial is similar but does not include block effects. Furthermore, only the drought stress was evaluated as an influencing variable. Thus, the model simplifies to

$$y_{klo} = \mu + r_k + t_{kl} + \rho_o + e_{klo} \quad (2)$$

where ρ_o corresponds to the o th drought stress level. In both models, VI's were added as a covariate for each of the nine combinations of leaf and position. As 16 VI were used, a total of 144 models each including different covariates were fitted. For all models, the error variance was estimated and used as evaluation criteria. It was assumed that a covariable, which correlates well with plant N content will reduce the error variance.

Error variances were stored and further analyzed with a generalized linear mixed model approach assuming a gamma distribution with a log link. The linear predictor was as follows:

$$\mu_{hpq} = \mu + l_p + p_q + (lp)_{pq} + i_h \quad (3)$$

where l_p is the effect of the p th leaf, p_q is the effect of the q th position, $(lp)_{pq}$ is the interaction effect of the p th leaf at the q th position, and i_h is the effect of the h th VI. The model allows accounting for overdispersion. If significant Wald tests were found, means were calculated using the inverse link function. For these means, a letter display was used to present the results of the Fishers LSD test created on the linked scale. All statistical evaluations were performed in the software environment SAS 9.4 by using the procedure PROC MIXED and PROC GLIMMIX.

3. Results

3.1. Nitrogen Trial

The chemically determined N content [%] showed significant differences ($p < 0.001$) and varied between 0.75% and 4.88% according to the implemented N treatments and growth stages in the N trial (Figure 4). The analysis of the residual error variance showed significant differences between leaf numbers and positions on the leaf. No significant differences were observed for the effects of the tested VI (Table 2; Figure 5). The interactions between leaf number and measurement position were found to have non-significant differences. Across all VIs, statistically significant lowest residual error variance was found at M3 and on leaf L1, and L3 (Figure 5). While the average residual error variances across VI were significantly different, almost no difference in error variance between leaf number and measurement position for the trait plant N content was observed (Figure 5).

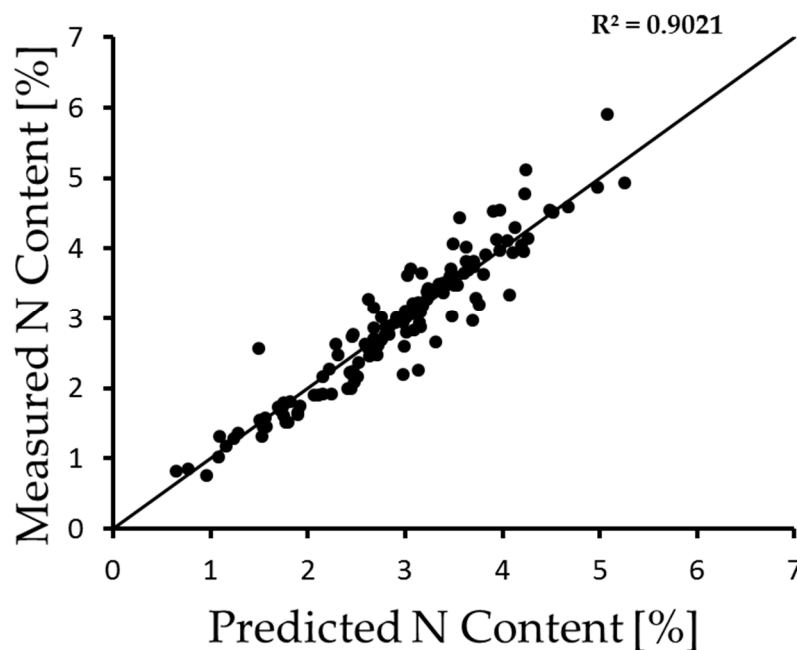
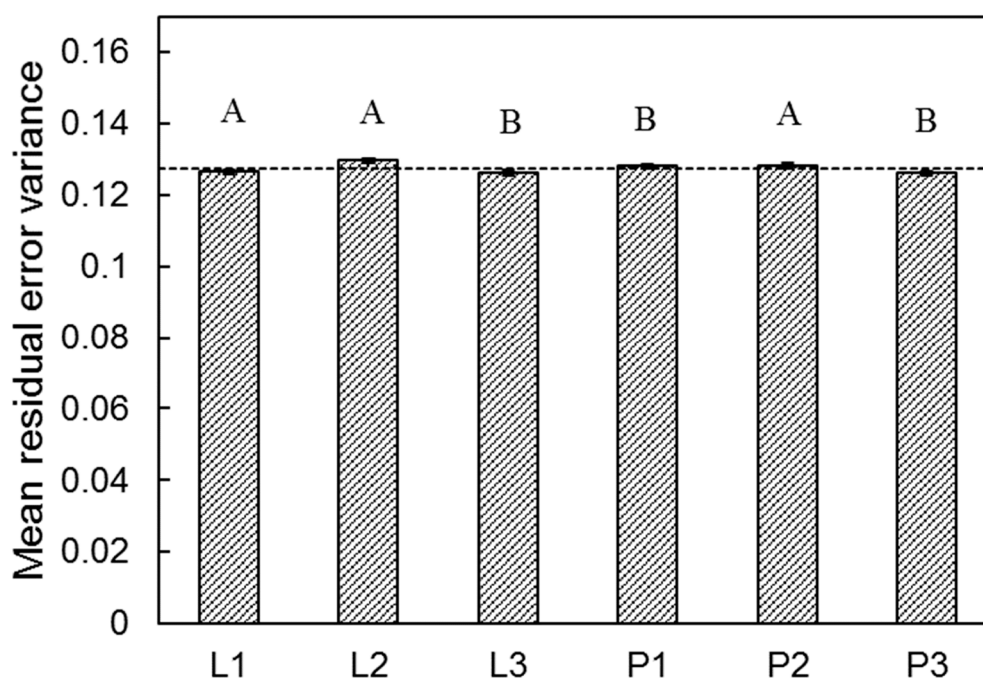


Figure 4. Scatter plot for measured and predicted nitrogen content of the nitrogen trial. The solid line indicates the 1:1.

Table 2. Results of the fixed effects of the statistical analyses of the nitrogen and drought stress trial. F values were rounded.

Effect	Nitrogen trial			Drought stress trial	
	DF	F value	Pr > F	F value	Pr > F
VI	15	0.49	0.9432	2.82	<0.0016
Leaf number	2	12.14	<0.0001	1.03	<0.3140
Position	2	4.34	<0.0152	1.84	<0.1657
Leaf number x Position	4	1.26	<0.2913	1.84	<0.1652

DF: degrees of freedom; Pr > F: probability level.

**Figure 5.** Mean residual error variance across VI (vegetation indices) of the nitrogen trial. L1 is considered the youngest fully developed leaf followed by the second L2 and third youngest leaf L3. P1 is the spectral reflectance measured at the leaf tip, P2 measured in the middle part of the leaf, and P3 represents the measurement taken at the leaf base of the respective leaf. The bars with the same letters within the leaves and within the positions show non-significant different residual error variances at $\alpha = 0.05$. The dotted line represents the residual error variance value without VI.

3.2. Drought Trial

Considering the drought trial (Table 2; Figure 6) where chemically determined N content varied due to the drought stress between 2.55% and 4.46%, the error variances showed significant differences ($p < 0.05$) only for VI and not for leaf number, position, and leaf number x position. Comparing the significance of different VI in the drought trial (Figure 6), the difference between PSRI, CropSpec, and BNI, indicated the highest mean residual error variance for PSRI, while BNI showed the lowest mean residual error variance.

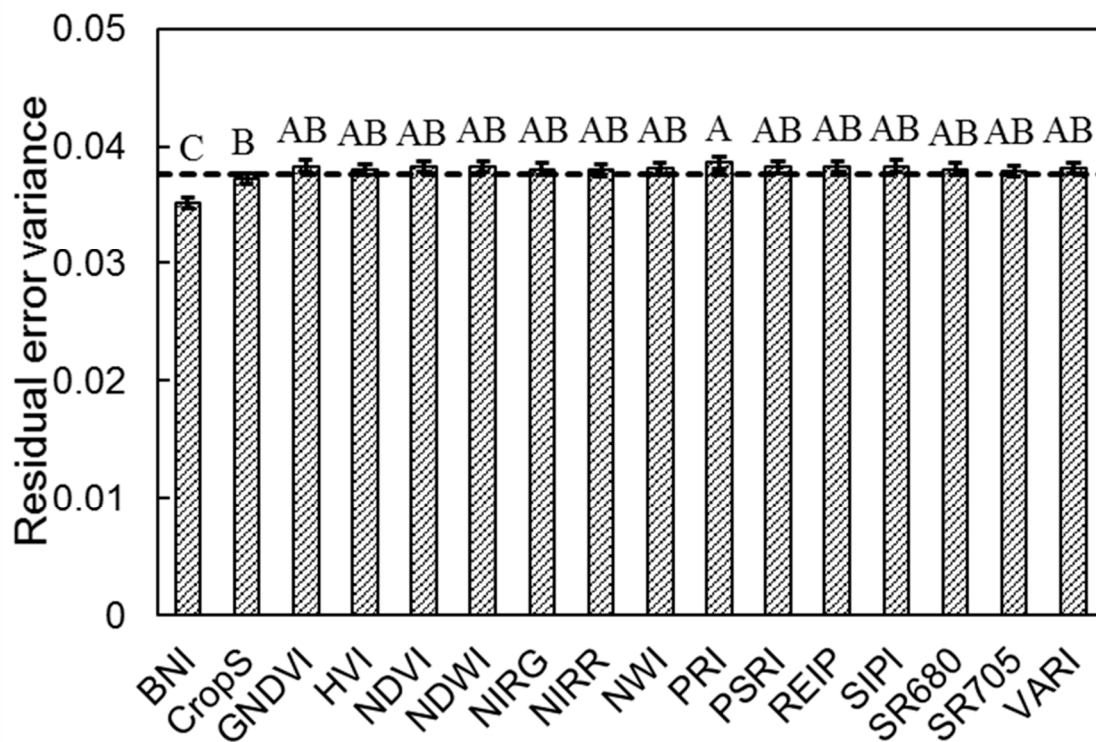


Figure 6. Different residual error variance for all used VI in the drought stress trial. The letters represent different significance groups. Indices with the same letters are not statistically different at a significance level of 0.05. The dotted line represents the residual value without using spectral reflectance measurements.

4. Discussion

This study evaluated the effect of a total of nine (three-leaf layers and three positions on each leaf) spectral reflection measurements on the prediction of N content (%) in wheat plants. To predict N content, spectral reflection measurements were used to calculate a range of published VI. Note that the aim of this study was not to optimize existing VIs, but rather to compare the nine input spectral reflection datasets and thus the impact of the leaf layer and measurement position on the accuracy of N prediction. Due to easy access and the common use of VIs in scientific and applied work [12,41,42], a range of 16 VI already published were used here. Note that each VI only used a few wavelengths. Thus, only a part of the information within the spectral reflection measurements was explored. More information can be explored when using a stepwise multiple linear regression (SMLR) and other full-spectral methods like partial least squares (PLS) [54]. These methods were tested in this study and came up with similar results as the ones presented in this paper.

Furthermore, other approaches can be used, like ridge regression [55] and neural networks [56,57], which can handle collinearity in regressions. Collinearity is common in spectral reflection data as wavelengths are measured within a narrow grid. All these alternative approaches can increase the predictability of absolute N content in plants. It was assumed that changes in absolute precision will not affect the ranking of the nine spectral reflection input measurements. This assumption was supported by results using a multiple regression approach and PLS on our data. Data are not shown here to avoid redirecting the focus of the manuscript from comparing the nine spectral reflection measurements to comparing approaches to convert wavelength measures into an N content prediction.

4.1. Leaf Number and Leaf Position

Spectral reflectance is used to detect differences in N content in plants non-destructively and to reveal the given heterogeneity in plant N supply within a field [58]. As the aim of this study was to predict plant N content within a field [42], e.g., for applying the right amount of fertilizer, effects of N level, growth stage, and drought were included in the statistical models. Thus, the statistical models can predict different N contents in plants within similar treatments averaged across these treatments. When dropping these treatment effects from the models, indices may explain well the difference between a trait (e.g., drought stress levels) not causally correlated with plant N. Note that VI explained more variance, if the treatment effect is excluded from the model. This was tested but not shown.

Considering the mixed model for all measurements in the N trial, a statistically significant higher mean residual error variance was given for L2 (Figure 5). Regarding the measurement position, a statistically significant lower value was given for the leaf base in the N trial, but differences were small. While differences were significant, they were not relevant, which was supported by the low differences between the significance groups (Figure 5). This conclusion was also reinforced by the drought stress trial, where no statistically significant difference between the leaf number and measurement position was shown. Different drought stress levels led to significantly different plant N contents. Gonzalez-Dugo et al. [59] also reported lower N contents for sunflower (*Helianthus annuus* L.) due to drought stress, based on the results of Alvarez de Toro [60]. They also showed plant N content under drought stress is dependent on the applied N. Low N application leads to a low change in plant N content, while high N application leads to a stronger plant N content reduction under drought stress. The wheat plants in this trial were cultivated under sufficient N supply, which can be seen as feasible to have significant differences between drought stress treatments.

To predict N content in wheat plants based on spectral measurements, reflectance can be measured at all positions on a leaf, at all leaves across different N treatments at different growth stages, as well as under drought stress.

4.2. Vegetation Indices and Wavelength

Regarding the residual error variance for all VI, significant differences were only determined in the drought trial for BNI (Figure 6). All other VI had no significant difference, especially the developed VI for water stress NDWI and NWI. In this trial, there was a reduction in plant N content due to drought stress observed, which was also reported by He and Dijkstra [61]. Therefore, these VI were used for the estimation of plant N under water-limited conditions. However, originally they have been developed for the estimation of water limitations in plants. In contrast, the BNI, which was developed for the estimation of plant N content showed the lowest residual error variance and seemed to be suitable for estimation of plant N content under water-limited conditions.

The BNI was the only VI out of 16 VI that used wavelengths from the blue part of the spectra. Tian et al., [43] successfully developed and tested this VI for estimation of leaf N canopy content in rice (*Oryza sativa* L.) and showed a linear relationship with canopy N content. Schlemmer et al. [62] tested different N levels in combination with drought stress in corn (*Zea mays* L.). They showed a weak influence of the reflectance spectrum under drought stress between 400 and 500 nm, if the plants were cultivated under sufficient N level. This could be the reason for the statistically lower residual error variance in the drought stress trial for all leaves and positions for BNI.

It is also important to mention that the selection criteria for the 16 VI used were based on literature, where VI were tested successfully for the determination of plant N content and drought stress [12,41,42,63,64].

This ensured that a broad range of different VI developed for N content and drought stress were tested, conceding, however, that there is a long list of VI that were not tested in the current study [32,49,65]. While we found no differences between VI in the N trial, we cannot preclude that there are no differences between VI at all. The drought stress showed the only significance for BNI, which means all VI except BNI performed in a similar way. The use of different VI sharing similar or identical wavelength ranges can be considered as not statistically independent. This can lead to the distortion of statistical results. Normally a broad range of VI focus on the red edge of the spectrum [66] leading to multiple uses of these wavelengths for calculation of various VI.

Several researchers evaluated the whole spectrum instead of using VI e.g., for plant disease detection [67] or canopy chlorophyll content [54]. These methods seem to be useful for further research where launches of hyperspectral satellite sensors are planned (e.g., EnMap, PRISMA) providing higher spectral resolution [68,69]. Other sensors like the Chinese HJ-1A [70] and the Indian Micro Satellite-1 (IMS-1) [71] also provide hyperspectral data, however, there is limited access for international scientists [69].

However current sensors including free available satellite images are normally limited to several wavelengths [72,73] and do not collect the whole spectrum in a spectral resolution like a spectrometer. This is mainly related to well tested and known VI's for the determination of N as well as a cost issue of the sensor and the necessary data processing to generate a final fertilizer recommendation. Using a spectrometer with a high spectral resolution, calculating existing VI's for nitrogen-based on the wavelength ranges seems to be a straight forward procedure to address if the differentiation between leaf and leaf positions based on existing VI's would be required.

4.3. Further Measurement Technologies, Limitations, and Future Applications

Hoel and Solhaug [74] tested the change of SPAD chlorophyll readings under shaded and fully illuminated conditions in wheat. Low changes were reported between shading and full illumination. This supports our finding of low differences between the three measured leaf layers, where L2 and L3 were shaded by L1. In comparison to spectrometer measurements, SPAD readings are limited to two wavelengths at 640 nm and 940 nm and are based on the principle of transmission of light [12]. Spectrometer readings, in contrast, focus on the reflectance of light. Comparisons of reflectance and SPAD values showed positive correlations for chlorophyll content, which also correlates very well with N content depending on different growth stages [75]. SPAD readings are contact measurements and not suitable for remote sensing applications [12].

Measuring leaf reflectance without separation of different leaves on canopy scale generally includes information of LAI, chlorophyll content or changes in plant morphology [76,77]. These lead to non-linear effects in the obtained sensor data and are not separated in commercialized products, which results in an overall mean N content [77]. Measuring at the canopy scale includes mixed information also from other parts of the plant like stem or leaf orientation [76], an aspect which was not considered in this study. It is also feasible, that differentiation between leaf layers is necessary under other nutrition deficiencies like sulfur, phosphorus, or potassium. Shaw and Royle [78] reported that early infection of lower leaf layers with *Septoria tritici* blotch (*Zymoseptoria tritici* D.) can make it necessary to differentiate between different leaves under leaf disease infections and has to be tested in further studies.

Currently, developed sensors are working on the canopy level and are not considering individual leaves or different positions on the leaf [79,80]. Nevertheless, we think, all these sensors require a minimum of spatial resolution in order to delineate the given within-field variability of plant N content on the farmer's practical scale (e.g., the width of sprayer bow). Hence, sensors for N fertilizer application in PF can only be useful if the spatial resolution of the sensor matches the N application size, which is determined by the fertilizer application technique. This has to be considered especially for satellite sensors, where spatial resolution ranges from 10–60 m [15]. Based on this study, differentiation between different leaf layers for the determination of N content can be seen as less relevant, which indicates valid measurements at the canopy scale.

5. Conclusions

The results of the study indicated that neither leaf number nor the measurement position on the leaf had an influence on the determination of plant N content, via spectral reflectance. Significant lower mean residual error variance (MREV) was found for leaves L1 and L3 and for measurement position on P3, but the difference of MREV between the leaves was very low and therefore considered as not relevant. While a broad range of different VI developed for the assessment of N content and drought stress was tested in this study, it cannot be excluded that there are no differences between VI at all and differences might exist for VI that were not tested in this study. To transfer the results to field measurements, it has to be considered that the measurements were taken under fully controlled lab conditions. Field measurements will be influenced by different effects like the reflection from soil, stem, or other plant parts, which can lead to weaker performance of spectral reflection measurements compared to lab conditions. In addition, other stress factors (e.g., diseases, other nutrient deficiencies) might occur in parallel in the field and interfere with spectral reflectance.

Author Contributions: Conceptualization, G.R., J.H., and S.G.-H.; methodology, G.R., J.H., and S.G.-H.; software, G.R. and J.H.; validation, G.R.; formal analysis, G.R.; investigation, G.R.; resources, G.R.; data curation, G.R.; writing—original draft preparation, G.R.; writing—review and editing, G.R., J.H., and S.G.-H.; visualization, G.R.; supervision, S.G.-H.; project administration, S.G.-H.; funding acquisition, S.G.-H.

Funding: This research was funded by the German Federal Environmental Foundation (DBU) (ProjectNr. 33143/01).

Acknowledgments: Many thanks to the hema electronic company for providing the spectrometer measurement equipment and Thomas Schwarzbäck for supporting the measurements and the device selection.

Conflicts of Interest: The authors declare no conflict of interest. The funders had no role in the design of the study; in the collection, analyses or interpretation of data; in the writing of the manuscript or in the decision to publish the results.

Appendix A

In the nitrogen trial, 140 plants were planted and harvested (Figures A1 and A2). As seven N fertilizer treatments were used, each N fertilizer treatment was applied to four pots; each pot contained five plants. Thus, the fertilizer treatment corresponded to the main plot factor and was allocated to pot according to the randomized complete block design. Within a pot, plants of different growth stages were tested. To generate plants of different growth stages, plants can be planted at different times and measured at a single harvest date or can be planted at the same time, but harvested at different time points. In both cases, the growth stage effect is confounded with the planting or harvest day. To handle this confounding, a more complex experimental design was used. The general idea behind this design was that planting date and harvest date were used as block factors. Within a block, as many growth stages as possible were measured. In our experiment, six planting dates and two harvest dates were used. This resulted in measuring plants of the same planting date at two different growth stages and measuring plants of five growth stages at the same harvest day (Figure A1).

With plants planted at six dates and harvested at two dates, five different growth stages can be observed. Thus, the design is complete as all growth stages occur in each pot. The experiment was performed as follows: wheat seeds were seeded at six different sowing dates (three weeks with two sowing dates per week) (Figure A2). Plants from the first sowing date were randomly planted to one of the positions within each pot of replicate 1 and 2. Thus, 14 plants were planted at the first planting date. Plants from the second sowing date were seeded randomly to one of the remaining positions in each pot of replicate 1 + 2, and to one position in replicate 3 + 4. Plants from the third, fourth, and fifth sowing dates were planted randomly to one of the remaining positions in each pot in replicate 1–4. Finally, plants from the sixth sowing date were seeded in the remaining positions of replicate 3 and 4. Note that plants of the first sowing date were 14 or 17 days older (two or two and a half week), compared to plants of the fifth or sixth sowing date, respectively. Furthermore, replicate 1 and 2 were measured and harvested first (H1) followed by replicates 3 and 4 half a week later (H2).

Thus, a plant sown at the third date measured at H1 has the same growth stage as a plant sown at the fourth sowing date and measured at H2 (indicated by the length of arrows in Figure A2).

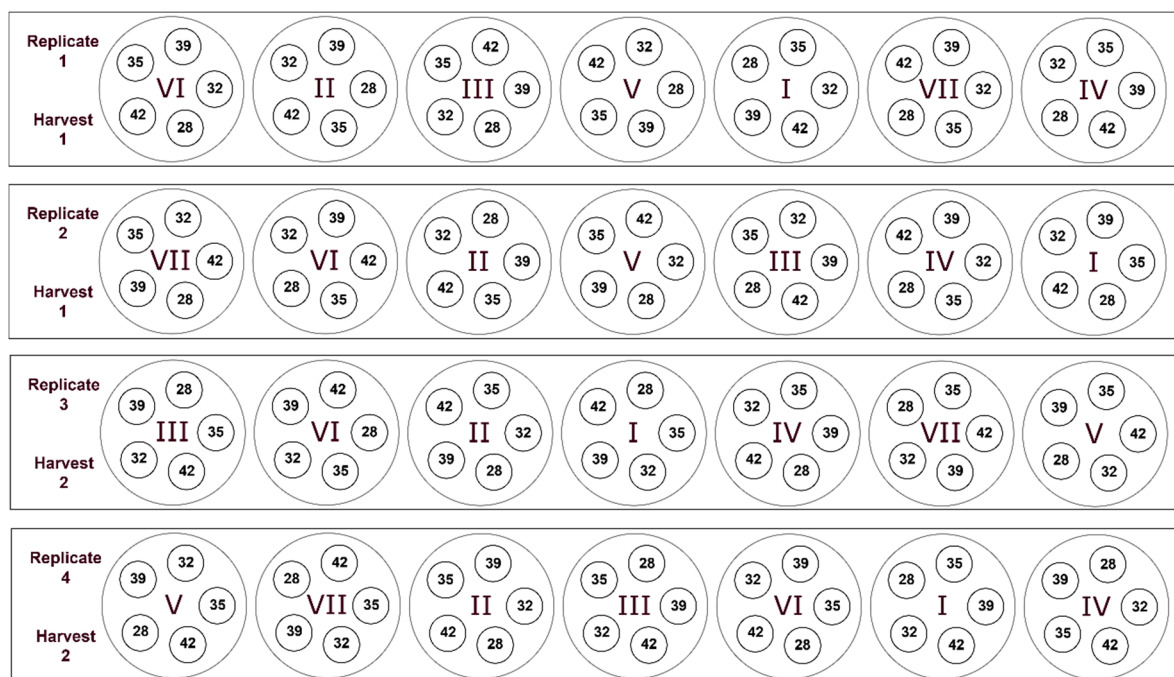


Figure A1. Experimental design of the nitrogen fertilizer trial. I–VII represents the pots for the corresponding nitrogen levels (0 mM N–2.0 mM N). Numbers 28–42 represents the growing days (from seeding until harvest) of the respective plant.

As mentioned above, the fertilizer treatment corresponded to the main plot factor and was allocated to pot according to the randomized complete block design. Growth stages were randomized to plants within a pot and thus can be seen as sub-plot factor. The design can be seen as a kind of split-plot design with two additional block factors (sowing date and harvest date). To model such type of data, the effects for both treatment factors (N treatment and growth stage) should be separated from the two blocking factors.

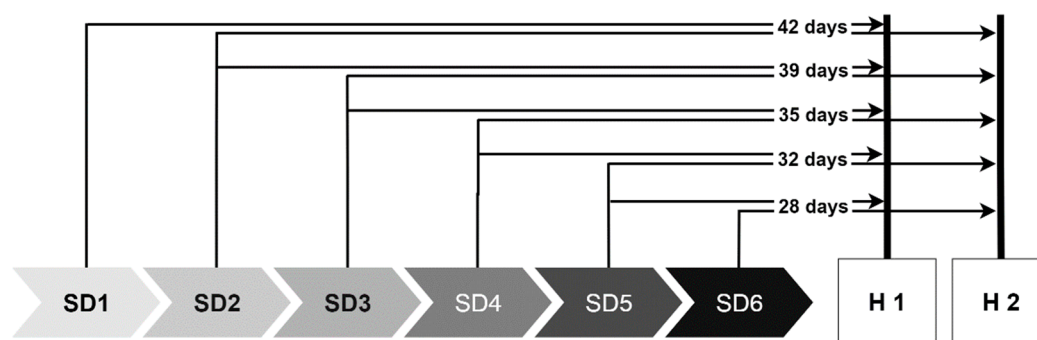


Figure A2. Scheme of different sowing dates (SD) and the corresponding harvest dates (H) of the nitrogen trial. The duration indicates the growing time (from sowing to harvest) in the experiment for each sowing date.

References

1. Ladha, J.K.; Pathak, H.; Krupnik, T.J.; Six, J.; Van Kessel, C. Efficiency of fertilizer nitrogen in cereal production: Retrospects and prospects. *Adv. Agron.* **2005**, *87*, 85–156.

2. Rafiqul, I.; Weber, C.; Lehmann, B.; Voss, A. Energy efficiency improvements in ammonia production—Perspectives and uncertainties. *Energy* **2005**, *30*, 2487–2504. [CrossRef]
3. Kim, H.; Kim, S.; Dale, B.E. Biofuels, Land Use Change, and Greenhouse Gas Emissions: Some Unexplored Variables. *Environ. Sci. Technol.* **2009**, *43*, 961–967. [CrossRef]
4. Gruber, N.; Galloway, J.N. An Earth-system perspective of the global nitrogen cycle. *Nature* **2008**, *451*, 293. [CrossRef]
5. Kim, S.; Dale, B.E. Effects of Nitrogen Fertilizer Application on Greenhouse Gas Emissions and Economics of Corn Production. *Environ. Sci. Technol.* **2008**, *42*, 6028–6033. [CrossRef]
6. European Commission. Directive 2000/60/EC of the European Parliament and of the Council of 23 October 2000 establishing a framework for Community action in the field of water policy. *Off. J. Eur. Union* **2000**, *327*, 193.
7. European Commission. Council Directive 91/676/EEC of 12 December 1991 concerning the protection of waters against pollution caused by nitrates from agricultural sources. *Off. J. Eur. Union* **1991**, *375*, 12.
8. Webber, H.; Heyd, V.; Horton, M.; Bell, M.; Matthews, W.; Chadburn, A. Precision farming and archaeology. *Archaeol. Anthropol. Sci.* **2019**, *11*, 727–734. [CrossRef]
9. Carter, L.M.; Rhoades, J.D.; Chesson, J.H. Mechanization of soil salinity assessment for mapping. *Am. Soc. Agric. Eng.* **1993**. Available online: https://www.ars.usda.gov/arsuserfiles/20360500/pdf_pubs/P1305.pdf (accessed on 8 September 2019).
10. Jackson, R.D.; Pinter, P.J. Spectral response of architecturally different wheat canopies. *Remote Sens. Environ.* **1986**, *20*, 43–56. [CrossRef]
11. Selige, T.; Böhner, J.; Schmidhalter, U. High resolution topsoil mapping using hyperspectral image and field data in multivariate regression modeling procedures. *Geoderma* **2006**, *136*, 235–244. [CrossRef]
12. Muñoz-Huerta, R.F.; Guevara-Gonzalez, R.G.; Contreras-Medina, L.M.; Torres-Pacheco, I.; Prado-Olivarez, J.; Ocampo-Velazquez, R.V. A Review of Methods for Sensing the Nitrogen Status in Plants: Advantages, Disadvantages and Recent Advances. *Sensors* **2013**, *13*, 10823–10843. [CrossRef] [PubMed]
13. Moran, M.S.; Inoue, Y.; Barnes, E.M. Opportunities and limitations for image-based remote sensing in precision crop management. *Remote Sens. Environ.* **1997**, *61*, 319–346. [CrossRef]
14. Mulla, D.J. Twenty five years of remote sensing in precision agriculture: Key advances and remaining knowledge gaps. *Biosyst. Eng.* **2013**, *114*, 358–371. [CrossRef]
15. Chemura, A.; Mutanga, O.; Odindi, J.; Kutuywayo, D. Mapping spatial variability of foliar nitrogen in coffee (*Coffea arabica* L.) plantations with multispectral Sentinel-2 MSI data. *ISPRS J. Photogramm. Remote Sens.* **2018**, *138*, 1–11. [CrossRef]
16. Hank, T.B.; Berger, K.; Bach, H.; Clevers, J.G.P.W.; Gitelson, A.; Zarco-Tejada, P.; Mauser, W. Spaceborne Imaging Spectroscopy for Sustainable Agriculture: Contributions and Challenges. *Surv. Geophys.* **2019**, *40*, 515–551. [CrossRef]
17. Xue, J.; Su, B. Significant Remote Sensing Vegetation Indices: A Review of Developments and Applications. *J. Sensors* **2017**, *2017*, 1–17. [CrossRef]
18. Thompson, A.L.; Thorp, K.R.; Conley, M.M.; Elshikha, D.M.; French, A.N.; Andrade-sanchez, P.; Pauli, D. Comparing Nadir and Multi-Angle View Sensor Technologies for Measuring in-Field Plant Height of Upland Cotton. *Remote Sens.* **2019**. [CrossRef]
19. Ramana, M.V.; Ramanathan, V.; Kim, D.; Roberts, G.C.; Corrigan, C.E. Albedo, atmospheric solar absorption and heating rate measurements with stacked UAVs. *Q. J. R. Meteorol. Soc.* **2007**, *133*, 1913–1931. [CrossRef]
20. Yao, H.; Huang, H. Remote sensing applications to precision farming. In *Remote Sensing of Natural Resources*; CRC Press: New York, NY, USA, 2013; pp. 333–352.
21. Bégué, A.; Todoroff, P.; Pater, J. Multi-time scale analysis of sugarcane within-field variability: Improved crop diagnosis using satellite time series? *Precis. Agric.* **2008**, *9*, 161–171. [CrossRef]
22. Baret, F.; Houlès, V.; Guérif, M. Quantification of plant stress using remote sensing observations and crop models: The case of nitrogen management. *J. Exp. Bot.* **2007**, *58*, 869–880. [CrossRef] [PubMed]
23. Link, A.; Reusch, S. Implementation of site-specific nitrogen application—Status and development of the YARA N-Sensor. *NJF Semin.* **2006**, *390*, 37–41.
24. Vigneau, N.; Ecartot, M.; Rabatel, G.; Roumet, P. Potential of field hyperspectral imaging as a non destructive method to assess leaf nitrogen content in Wheat. *Field Crop. Res.* **2011**, *122*, 25–31. [CrossRef]

25. Thomasson, J.A.; Sui, R.; Cox, M.S.; Al-Rajehy, A. Soil reflectance sensing for determining soil properties in precision agriculture. *Trans. ASAE* **2001**, *44*, 1445. [[CrossRef](#)]
26. Haboudane, D.; Miller, J.R.; Tremblay, N.; Zarco-Tejada, P.J.; Dextraze, L. Integrated narrow-band vegetation indices for prediction of crop chlorophyll content for application to precision agriculture. *Remote Sens. Environ.* **2002**, *81*, 416–426. [[CrossRef](#)]
27. Sripada, R.P.; Heiniger, R.W.; White, J.G.; Weisz, R. Aerial Color Infrared Photography for Determining Late-Season Nitrogen Requirements in Corn. *Agron. J.* **2005**, *97*, 1443. [[CrossRef](#)]
28. Schepers, J.S.; Francis, D.D.; Vigil, M.; Below, F.E. Comparison of corn leaf nitrogen concentration and chlorophyll meter readings. *Commun. Soil Sci. Plant Anal.* **1992**, *23*, 2173–2187. [[CrossRef](#)]
29. Thenkabail, P.S.; Smith, R.B.; De Pauw, E. Hyperspectral Vegetation indices and their relationships with agricultural crop characteristics. *Remote Sens. Environ.* **2000**, *71*, 158–182. [[CrossRef](#)]
30. Gitelson, A.A. Wide Dynamic Range Vegetation Index for Remote Quantification of Biophysical Characteristics of Vegetation. *J. Plant Physiol.* **2004**, *161*, 165–173. [[CrossRef](#)]
31. Haboudane, D.; Tremblay, N.; Miller, J.R.; Vigneault, P. Remote Estimation of Crop Chlorophyll Content Using Spectral Indices Derived From Hyperspectral Data. *IEEE Trans. Geosci. Remote Sens.* **2008**, *46*, 423–437. [[CrossRef](#)]
32. Li, F.; Miao, Y.; Hennig, S.D.; Gnyp, M.L.; Chen, X.; Jia, L.; Bareth, G. Evaluating hyperspectral vegetation indices for estimating nitrogen concentration of winter wheat at different growth stages. *Precis. Agric.* **2010**, *11*, 335–357. [[CrossRef](#)]
33. Bertheloot, J.; Andrieu, B.; Martre, P. Light–nitrogen relationships within reproductive wheat canopy are modulated by plant modular organization. *Eur. J. Agron.* **2012**, *42*, 11–21. [[CrossRef](#)]
34. Wang, Z.; Wang, J.; Zhao, C.; Zhao, M.; Huang, W.; Wang, C. Vertical Distribution of Nitrogen in Different Layers of Leaf and Stem and Their Relationship with Grain Quality of Winter Wheat. *J. Plant Nutr.* **2005**, *28*, 73–91. [[CrossRef](#)]
35. Wang, Z. Prediction of Canopy Nitrogen Distribution and Grain Quality Using Remote Sensing in Winter Wheat (*Triticum aestivum* L.). Ph.D. Thesis, China Agricultural University, Beijing, China, 2004.
36. Zhao, C.J.; Huang, W.J.; Wang, J.H.; Liu, L.Y.; Song, X.Y.; Ma, Z.H.; Li, C. Extracting winter wheat chlorophyll concentration vertical distribution based on bidirectional canopy reflected spectrum. *Trans. Chin. Soc. Agric. Eng.* **2006**, *22*, 104–109.
37. Gara, T.W.; Skidmore, A.K.; Darvishzadeh, R.; Wang, T. Leaf to canopy upscaling approach affects the estimation of canopy traits. *GIScience Remote Sens.* **2019**, *56*, 554–575. [[CrossRef](#)]
38. Hoagland, D.R.; Arnon, D.I. The water-culture method for growing plants without soil. *Circ. Calif. Agric. Exp. Stn.* **1950**, *347*, 32.
39. Zadoks, J.C.; Chang, T.T.; Konzak, C.F. A decimal code for the growth stages of cereals. *Weed Res.* **1974**, *14*, 415–421. [[CrossRef](#)]
40. Dumas, A. Stickstoffbestimmung nach Dumas (N-determination according to Dumas). In *Die Praxis des Organischen Chemikers*; Gattermann, L., Wieland, H., Eds.; De Gruyter: Berlin, Germany, 1962; pp. 45–51.
41. Sims, D.A.; Gamon, J.A. Relationships between leaf pigment content and spectral reflectance across a wide range of species, leaf structures and developmental stages. *Remote Sens. Environ.* **2002**, *81*, 337–354. [[CrossRef](#)]
42. Zecha, C.; Link, J.; Claupein, W. Fluorescence and Reflectance Sensor Comparison in Winter Wheat. *Agriculture* **2017**, *7*, 78. [[CrossRef](#)]
43. Tian, Y.C.; Yang, J.; Yao, X.; Zhu, Y.; Cao, W.X. A newly developed blue nitrogen index for estimating canopy leaf nitrogen concentration of rice. *Chin. J. Appl. Ecol.* **2010**, *24*, 966–972.
44. Reusch, S.; Jasper, J.; Link, A. Estimating crop biomass and nitrogen uptake using CropSpec TM, a newly developed active crop-canopy reflectance sensor. In Proceedings of the 10th International Conference on Precision Agriculture, Denver, CO, USA, 18–21 July 2010.
45. Gitelson, A.A.; Kaufman, Y.J.; Merzlyak, M.N. Use of a Green Channel in Remote Sensing of Global Vegetation from EOS-MODIS. *Remote Sens. Environ.* **1996**, *58*, 289–298. [[CrossRef](#)]
46. Rouse, W.; Haas, H.; Schell, J.; Deering, D. Monitoring vegetation systems in the great plains with ERTS. In Proceedings of the 3rd ERTS Symposium; NASA SP-351. Freden, S.C., Becker, M.A., Eds.; NASA: Washington, DC, USA, 1973; pp. 309–317.

47. Gao, B. NDWI—A normalized difference water index for remote sensing of vegetation liquid water from space. *Remote Sens. Environ.* **1996**, *58*, 257–266. [[CrossRef](#)]
48. Bausch, W.C.; Duke, R.H. Remote Sensing of Plant Nitrogen Status in Corn. *Trans. ASAE* **1996**, *39*, 1869–1875. [[CrossRef](#)]
49. Babar, M.A.; Reynolds, M.P.; van Ginkel, M.; Klatt, A.R.; Raun, W.R.; Stone, M.L. Spectral Reflectance to Estimate Genetic Variation for In-Season Biomass, Leaf Chlorophyll, and Canopy Temperature in Wheat. *Crop Sci.* **2006**, *46*, 1046. [[CrossRef](#)]
50. Peñuelas, J.; Gamon, J.A.; Fredeen, A.L.; Merino, J.; Field, C.B. Reflectance Indices Associated with Physiological Changes in Nitrogen-and Water-Limited Sunflower Leaves. *Remote Sens. Environ.* **1994**, *146*, 135–146. [[CrossRef](#)]
51. Merzlyak, M.N.; Gitelson, A.A.; Chivkunova, O.B.; Yu, V.; Campus, S.B. Non-destructive optical detection of pigment changes during leaf senescence and fruit ripening. *Physiol. Plant.* **1999**, *106*, 135–141. [[CrossRef](#)]
52. Horler, D.N.H.; Dockray, M.; Barber, J. The red edge of plant leaf reflectance. *Int. J. Remote Sens.* **1983**, *4*, 273–288. [[CrossRef](#)]
53. Kaufman, Y.J.; Tanrd, D. Strategy for Direct and Indirect Methods for Correcting the Aerosol Effect on Remote Sensing: From AVHRR to EOS-MODIS. *Remote Sens. Environ.* **1992**, *55*, 65–79. [[CrossRef](#)]
54. Atzberger, C.; Guérif, M.; Baret, F.; Werner, W. Comparative analysis of three chemometric techniques for the spectroradiometric assessment of canopy chlorophyll content in winter wheat. *Comput. Electron. Agric.* **2010**, *73*, 165–173. [[CrossRef](#)]
55. Hoerl, A.E.; Kennard, R.W. Ridge Regression: Biased Estimation for Nonorthogonal Problems. *Technometrics* **1970**, *12*, 55–67. [[CrossRef](#)]
56. Haykin, S. *Neural Networks: A Comprehensive Foundation*; Macmillan College Publishing: Englewood Cliffs, NJ, USA, 1994; ISBN 0023527617.
57. Sarle, W.S. Neural Networks and Statistical Models. In Proceedings of the 19th Annual SAS Users Groups International Conference, Cary, NC, USA; 1994; pp. 1538–1550.
58. Thorp, K.R.; Wang, G.; Bronson, K.F.; Badaruddin, M.; Mon, J. Hyperspectral data mining to identify relevant canopy spectral features for estimating durum wheat growth, nitrogen status, and grain yield. *Comput. Electron. Agric.* **2017**, *136*, 1–12. [[CrossRef](#)]
59. Gonzalez-Dugo, V.; Durand, J.L.; Gastal, F. Water deficit and nitrogen nutrition of crops. *Sustain. Agric.* **2009**, *2*, 557–575. [[CrossRef](#)]
60. De Toro, A. *Respuesta del Girasol (Helianthus annuus L.) a un Suministro Variable de Agua de Riego y de Nitrogeno*; University of Cordoba: Cordoba, Spain, 1987.
61. He, M.; Dijkstra, F.A. Drought effect on plant nitrogen and phosphorus: A meta-analysis. *New Phytol.* **2014**, *204*, 924–931. [[CrossRef](#)] [[PubMed](#)]
62. Schlemmer, M.R.; Francis, D.D.; Shanahan, J.F.; Schepers, J.S. Remotely Measuring Chlorophyll Content in Corn Leaves with Differing Nitrogen Levels and Relative Water Content. *Agron. J.* **2005**, *97*, 106. [[CrossRef](#)]
63. Hansen, P.M.; Schjoerring, J.K. Reflectance measurement of canopy biomass and nitrogen status in wheat crops using normalized difference vegetation indices and partial least squares regression. *Remote Sens. Environ.* **2003**, *86*, 542–553. [[CrossRef](#)]
64. Zhao, D.; Huang, L.; Li, J.; Qi, J. A comparative analysis of broadband and narrowband derived vegetation indices in predicting LAI and CCD of a cotton canopy. *ISPRS J. Photogramm. Remote Sens.* **2007**, *62*, 25–33. [[CrossRef](#)]
65. Hatfield, J.L.; Gitelson, A.A.; Schepers, J.S.; Walthall, C.L. Application of spectral remote sensing for agronomic decisions. *Agron. J.* **2008**, *100*, 117–131. [[CrossRef](#)]
66. Antille, D.L.; Lobsey, C.R.; McCarthy, C.L.; Thomasson, J.A.; Baillie, C.P. A review of the state of the art in agricultural automation. Part IV: Sensor-based nitrogen management technologies. In *An ASABE Meeting Presentation, Proceedings of the Annual International Meeting, Detroit, MI, USA, 29 July–1 August 2018*; American Society of Agricultural and Biological Engineers: St. Joseph, MI, USA, 2018.
67. Thomas, S.; Wahabzada, M.; Kuska, M.T.; Rascher, U.; Mahlein, A.-K. Observation of plant–pathogen interaction by simultaneous hyperspectral imaging reflection and transmission measurements. *Funct. Plant Biol.* **2017**, *44*, 23. [[CrossRef](#)]

68. Labate, D.; Ceccherini, M.; Cisbani, A.; De Cosmo, V.; Galeazzi, C.; Giunti, L.; Melozzi, M.; Pieraccini, S.; Stagi, M. The PRISMA payload optomechanical design a high performance instrument for a new hyperspectral mission. In Proceedings of the 59th International Astronautical Congress IAC, Glasgow, UK, 29 September–3 October 2008; pp. 2637–2643. [[CrossRef](#)]
69. Guanter, L.; Kaufmann, H.; Segl, K.; Foerster, S.; Rogass, C.; Chabrillat, S.; Kuester, T.; Hollstein, A.; Rossner, G.; Chlebek, C.; et al. The EnMAP spaceborne imaging spectroscopy mission for earth observation. *Remote Sens.* **2015**, *7*, 8830–8857. [[CrossRef](#)]
70. Zhao, X.; Xiao, Z.; Kang, Q.; Li, Q.; Fang, L. Overview of the Fourier Transform Hyperspectral Imager (HSI) boarded on HJ-1A satellite. *2010 IEEE International Geosci. Remote Sens. Symp.* **2010**, 4272–4274. [[CrossRef](#)]
71. Kumar, A.; Saha, A.; Dadhwal, V.K. Some issues related with sub-pixel classification using HYSI data from IMS-1 satellite. *J. Indian Soc. Remote Sens.* **2010**, *38*, 203–210. [[CrossRef](#)]
72. Platnick, S.; King, M.D.; Ackerman, S.A.; Menzel, W.P.; Baum, B.A.; Riédi, J.C.; Frey, R.A. The MODIS cloud products: Algorithms and examples from terra. *IEEE Trans. Geosci. Remote Sens.* **2003**, *41*, 459–472. [[CrossRef](#)]
73. Forkuor, G.; Dimobe, K.; Serme, I.; Tondoh, J.E. Landsat-8 vs. Sentinel-2: Examining the added value of sentinel-2's red-edge bands to land-use and land-cover mapping in Burkina Faso. *GIScience Remote Sens.* **2018**, *55*, 331–354. [[CrossRef](#)]
74. Hoel, B.O.; Solhaug, K. Effect of Irradiance on Chlorophyll Estimation with the Minolta SPAD-502 Leaf Chlorophyll Meter. *Ann. Bot.* **1998**, *82*, 389–392. [[CrossRef](#)]
75. Zhou, G.; Yin, X. Assessing nitrogen Nutritional status, Biomass and Yield of Cotton with NDVI, SPAD and Petiole SAP Nitrate concentration. *Exp. Agric.* **2018**, *54*, 531–548. [[CrossRef](#)]
76. Schepers, J.; VanToai, T.; Major, D.J.; Baumeister, R.; Touré, A.; Zhao, S. Methods of Measuring and Characterizing the Effects of Stresses on Leaf and Canopy Signatures. *ASA Spec. Publ.* **2003**, *66*, 81–93. [[CrossRef](#)]
77. Li, H.; Zhao, C.; Huang, W.; Yang, G. Non-uniform vertical nitrogen distribution within plant canopy and its estimation by remote sensing: A review. *Field Crop. Res.* **2013**, *142*, 75–84. [[CrossRef](#)]
78. Shaw, M.W.; Royle, D.J. Estimation and validation of a function describing the rate at which Mycosphaerella graminicola causes yield loss in winter wheat. *Ann. Appl. Biol.* **1989**, *115*, 425–442. [[CrossRef](#)]
79. Rodriguez-Moreno, F.; Zemek, F.; Kren, J.; Píkl, M.; Lukas, V.; Novak, J. Spectral monitoring of wheat canopy under uncontrolled conditions for decision making purposes. *Comput. Electron. Agric.* **2016**, *125*, 81–88. [[CrossRef](#)]
80. Filella, I.; Serrano, L.; Serra, J.; Penuelas, J. Evaluating Wheat Nitrogen Status with Canopy Reflectance Indices. *Crop Sci.* **1995**, *35*, 1400–1405. [[CrossRef](#)]

